Comparative Studies on Combustion of Peanut and Tamarind Shells in a Bubbling Fluidized Bed: Combustion and Emission Characteristics

Porametr Arromdee, Vladimir I. Kuprianov*, Methawi Nithikan, Nonthawat Wongjaturapat, Ramajitti Pasutnavin, Thawin Tilokkul, Veratat Thamrongdullapark, Wallop Lamlertpongpana

School of Manufacturing Systems and Mechanical Engineering, Sirindhorn International Institute of Technology, Thammasat University, Pathum Thani 12121, Thailand

* Corresponding Author. E-mail: ivlaanov@siit.tu.ac.th; Tel: (+662) 986 9009, ext. 2208; Fax: (+662) 986 9112

Abstract

This paper presents the experimental results from a study of burning shredded peanut/tamarind shells in a bubbling fluidized-bed combustor with a cone-shape bed using alumina sand as the inert bed material. For both fuel options, the combustion tests were performed at the fuel feedrate of about 60 kg/h, when ranging excess air from about 20% to 80%. During each test run, temperature and concentrations of O_2, CO, C_xH_y (as CH_4) and NO were measured along the axial direction in the reactor as well as at stack. The axial temperature profiles in the reactor were found to be rather uniform and weakly affected by the fuel type and excess air. However, the axial profiles of distinct gaseous species showed similar trends for the two fuels with substantial effects from the fuel properties and operating conditions. The CO and C_xH_y emissions of the combustor can be effectively controlled via maintaining excess air. With increasing excess air, the NO emission was found to be increased remaining, nevertheless, at a level below the national NO emission limit. For the range of operating conditions, the combustion efficiency was found to be high, 97.6%–99.8%, when burning peanut/tamarind shells as shredded fuels in this conical fluidized-bed combustor.

Keywords*:* Peanut/tamarind shells; Conical fluidized-bed combustor; Emissions; Combustion efficiency.

1. Introduction

Peanuts and tamarind are popular food products in Thailand and many other countries around the world. Peanut and tamarind shells are the major byproducts (residues) from peanuts and tamarind processing, collected on a large scale in agricultural and food sectors. With the calorific value of 16–17 MJ/kg, these residues indicate therefore high potentials to be used as fuel in direct combustion systems.

The fluidized bed-combustion technology is proven to be the effective technology for energy conversion from various biomasses. A large number of studies have been devoted to bubbling, vortexing and circulating fluidized-bed combustion systems firing conventional (viable) biomass fuels, such as rice husk, sugar cane bagasse and woody residues [1–5]. Some authors pointed at difficulties in achieving high combustion efficiency when firing high-ash biomass fuels [2,3], while the others highlighted

ash-related operational problems caused by alkali-based compounds in biomass ashes [1]. These studies revealed that the combustion efficiency and emissions of a biomass-fuelled system depend on the system's design features and operating conditions, as well as on physical and chemical properties of fuel burned.

During the past decade, a growing attention has been paid to a feasibility of effective utilization of various unconventional biomass fuels, from fibrous fuels to fruit stones and nut/fruit shells, manly through their burning in bubbling or circulating fluidized-bed combustion systems. As shown in some pioneering studies, combustion efficiency of systems firing such fuels is comparatively low and strongly influenced by fuel properties, whereas gaseous emissions from these systems can be controlled at a level typical for conventional fuels [6–8]. Some other research works revealed an elevated risk of bed agglomeration and defluidization, generally caused by alkali-based mineral compounds, especially when using silica sand as the inert bed material in a fluidized-bed combustion system. To prevent the bed agglomeration, some alternative bed materials, such as alumina and aluminum-rich materials, as well as dolomite and limestone, can be used for firing high-alkali biomass fuels in a fluidized bed [1,9].

The main objective of this work was to investigate the combustion and emission characteristics of firing peanut/tamarind shells in the conical fluidized-bed combustor (referred to as 'conical FBC') using alumina sand as the inert bed material. Effects of fuel properties and operating conditions (excess air) on formation and decomposition of gaseous pollutants (CO, C_xH_y as CH_4, and NO) in different regions of the combustor as well as on combustion efficiency and gaseous emissions of the combustor were the main focus of this study.

2. Methodology

2.1 Experimental set-up

Fig. 1 shows the schematic diagram of an experimental set-up with the conical FBC used in this study. The combustor consisted of six refractory-lined steel modules connected coaxially: a conical module with cone angle of 40° and inner diameter of 0.25 m at the bottom plane, and five cylindrical modules with height of 0.5 m and inner diameter of 0.9 m. In each module, the refractory-cement insulation was 50 mm thick, lined inside 4.5-mm-thick steel walls. The modules had gas sampling ports, as well as stationary Chromel-Alumel thermocouples (of type K), the latter being used to measure temperature (with the accuracy of ±1%) in the axial direction inside the rector during the combustor start-up and testing.

Alumina sand with a solid density of about 3400 kg/m^3 and particle sizes 0.3–0.5 mm was used as the inert bed material in all experiments. Table 1 shows the chemical composition (as oxides, wt.%) of the bed material. It can be seen in Table 1 that Al_2O_3 was the major component in this sand. Beside the oxides listed in Table 1, the sand also included small proportions of ZrO_2, Na_2O, BaO and P_2O_5, as well as some other oxides of negligible wt.%. In all test runs, the static bed height of alumina sand was fixed at 30 cm. The above-mentioned particle size and static bed height of the inert bed material along with the

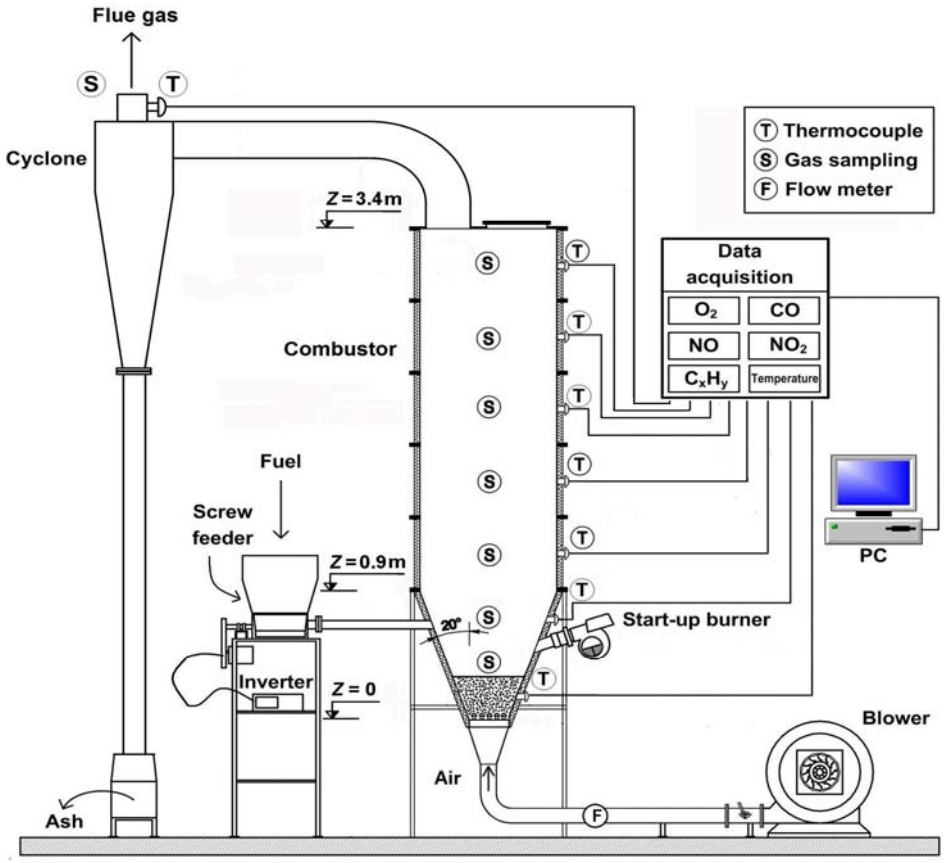

Fig. 1 Schematic diagram of the experimental set-up with the conical FBC.

selected cone angle ensured stable bubbling fluidized-bed regime in this conical FBC [10].

A 25-hp blower delivered air to the conical FBC. The air was injected into the bed through a 13-bubble-cap air distributor, which generated a fluidized bed at the combustor bottom. A diesel start-up burner (from Riello Burners Co.) was used to preheat alumina sand prior to experiments. The burner was fixed at a 0.5 m level above the air distributor and inclined at a –30° angle to the horizontal. When the bed temperature reached about 700 °C, the burner diesel pump was turned off. However, during combustion tests, a burner fan continued to operate in order to protect the burner's nozzle head against overheating. In the meantime, a rectangular steel plate with dimensions of 20 cm × 30 cm × 0.5 cm was used to screen the burner from the combustor space and, thus, avoid the impact of a flame onto the burner.

Table 1. Chemical composition of alumina sand (wt.%) used as the inert bed material in the conical FBC when firing biomass fuels.

SiO_2	Al_2O_3	Fe_2O_3	TiO_2	CaO	MgO	K_2O
3.46±0.07	92.42±2.59	0.66 ±0.02	2.74 ±0.01	0.72± 0.02	0.18± 0.03	0.11±0.02

Table 2. Properties of peanut and tamarind shells used in experimental tests on the conical FBC.

Biomass fuels	Ultimate analysis (wt.%, as-received basis)						Proximate analysis (wt.%, as-received basis)				
	C	H	O	N	S		W	A	VM	FC	LHV (kJ/kg)
Peanut shells	48.10	5.48	30.05	1.30	0.08		9.3	5.7	65.4	19.6	16,400
Tamarind shells	47.70	5.24	34.98	0.56	0.02		8.6	2.9	66.8	21.7	16,300

A screw-type feeder delivered each of the tested biomass fuels over the bed at a level Z = 0.6 m above the air distributor (see Fig. 1). The rotational speed of the screw feeder was adjusted using a three-phase inverter. A cyclone installed downstream from the combustor was used to remove ash particulates from a flue gas.

2.2 The fuels

Table 2 shows the ultimate and proximate analyses, as well as the lower heating value (LHV) of peanut and tamarind shells used in this experimental study. It can be seen in Table 2 that both biomass fuels were characterized by a significant amount of volatile matter (VM), a moderate proportion of fixed carbon (FC), and relatively low contents of fuel-moisture (W) and fuel-ash (A) in the proximate analysis, which resulted in a substantial LHV of both fuels. Note that the peanut shells contained a much higher proportion of fuel-N (1.30 wt.%) than tamarind shells (0.56 wt.%). Due quite low fuel-S (less than 0.1 wt.%), SO_2 was not addressed in this study.

Preliminary tests on the combustor for firing peanut and tamarind shells with original (coarse) fuel particles showed serious problems in fuel feeding, which resulted in substantial time-domain fluctuations of combustion and emission characteristics and (sometimes) unstable operation of the reactor. It was therefore decided to burn the shells as shredded fuels. Note that the shape and size of the shredded peanut and tamarind shells were quite irregular: from fine sawdust-like particles to flake-shape particles with the maximum sieve size of about 5 mm. The solid density of both biomass fuels was experimentally estimated to be: 580±20 kg/m^3 for peanut shells, and 420±15 kg/m^3 for tamarind shells.

2.3 Experimental procedure

In all the test runs for individual firing peanut and tamarind shells, the fuel feedrate (FR) was maintained at about 60 kg/h. Thus, taking into account the fuel LHVs, the heat input to the combustor was nearly the same, approximately 270 kW_{th}, for the two fuels. For each fuel option, excess air (EA) was variable and specified at values of 20%, 40%, 60% and 80%.

To investigate the behavior of temperature and gas concentrations (O_2, CO, C_xH_y as CH_4, and NO) in different regions of the reactor, these variables were measured in each test run (for the selected combustor load and excess air) along the combustor centerline, at seven levels above the air distributor. To quantify the gaseous emissions (CO, C_xH_y as CH_4, and NO) from the conical FBC, measurements were performed at the cyclone

exit as well. A model "Testo-350XL" gas analyzer (Testo, Germany) was used to monitor the temperature and gas concentrations. The measurement accuracies were ±0.5% for the temperature (using the Type K thermocouples), ±5% for CO in the range of 100–2000 ppm, ±10% for CO higher than 2000 ppm, ±10% for C_xH_y (as CH_4) up to 40,000 ppm, ±5% for NO, and ±0.2% (by vol.) for O_2.

For each test run, EA was quantified by Ref. [11] using the O_2, CO and C_xH_y (as CH_4) concentrations at the cyclone exit. Heat loss due to unburned carbon and that due to incomplete combustion (both, as percentages of LHV) were predicted together with the combustion efficiency according to Ref. [12]. The unburned carbon content in fly ash was determined in laboratory tests with the aim to quantify the associated heat loss, whereas the heat loss due to incomplete combustion was predicted based on the CO and C_xH_y (as CH_4) emissions using relevant parameters (EA, LHV and the volume of "dry" flue gas).

3. Results and Discussion

3.1 Axial temperature and gas concentration profiles in the conical FBC

Fig. 2 shows the axial temperature and O_2 concentration profiles in the conical FBC for firing shredded peanut/tamarind shells at the fuel feed rate of about 60 kg/h for the range of EA. For the two biomass fuels, the axial profiles of both temperature and O_2 concentration were found to exhibit similar trends.

It can be seen in Fig. 2 that in the bottom part of the combustor (at $0 < Z < 1$ m), including the dense and splash zones of the bed as well as some portion of the freeboard, the

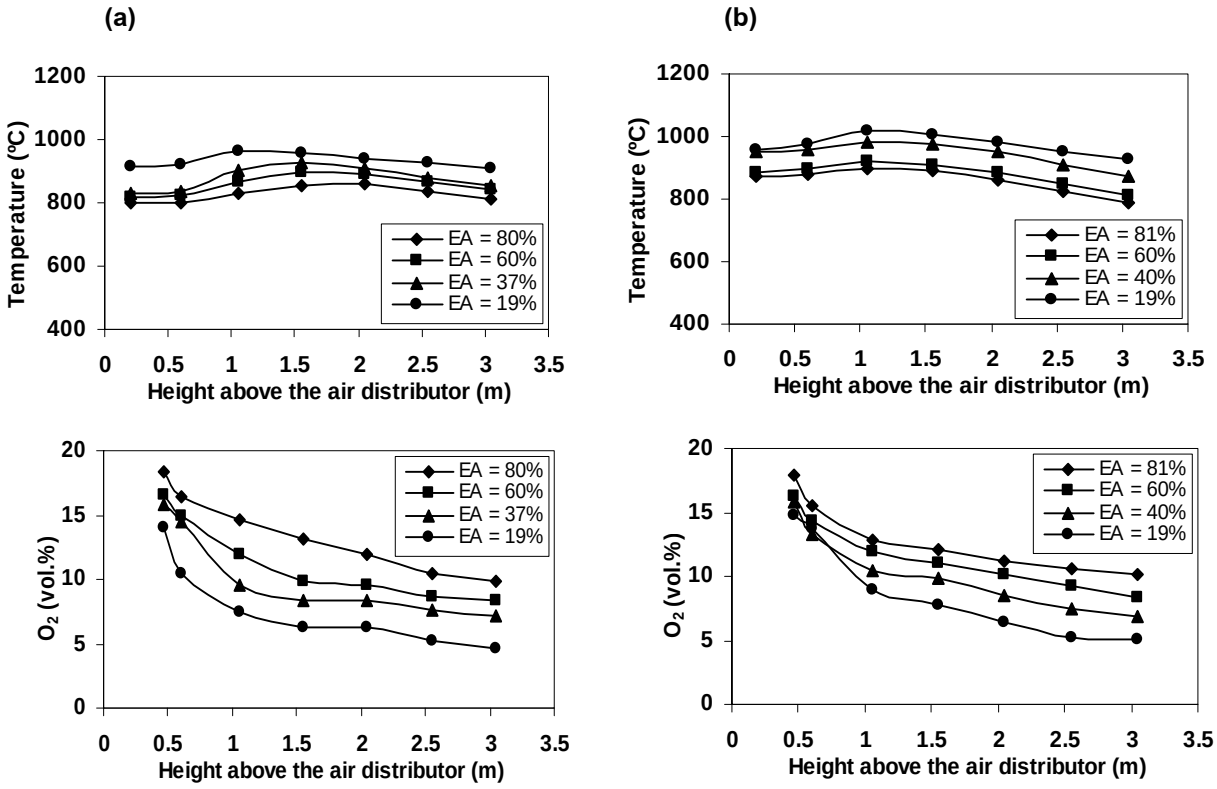

Fig. 2 Effects of excess air on the axial temperature and O_2 concentration profiles in the conical FBC when firing 60 kg/hr of (a) peanut shells and (b) tamarind shells.

axial temperature profiles were characterized by a slight positive gradient in the axial direction, mainly due to the over-bed fuel feeding and also endothermic processes of drying and devolatilization of fuel particles. In the upper region of the reactor (Z > 1 m), the temperature was found to be slightly reduced with higher Z because of the heat loss across the combustor walls. At any fixed point (or level Z above the air distributor), an increase in EA resulted in some reduction of the temperature, apparently caused by the air dilution effects. At all the locations along the combustor centerline, the temperature for firing peanut shells was close (within a relative difference of 2–10%) to that for firing tamarind shells at similar EA, mainly due to identical heat inputs.

In all the test runs, the axial O_2 concentration diminished gradually along the reactor height. As seen in Figs. 2a and 2b, a significant proportion of O_2 was consumed in the bottom part of the combustor when firing the fuels. However, the rate of O_2 consumption in this region for firing peanut shells was apparently higher than that for burning tamarind shells. This result can be explained by a porous texture of peanut shells (with a well-developed internal surface), leading to a higher reactivity of peanut shell coarse particles compared to that of tamarind shell particles (with no porosity) of similar size. Yet, due to the higher solid density, a greater proportion of peanut shell particles likely penetrated into the dense bed than that of tamarind shell particles. In the upper region, the O_2 drop along the centerline occurred at a rather low rate, the latter being somewhat higher when burning tamarind shells. This fact pointed at a higher carryover of tamarind shell chars and volatiles into the freeboard compared to that for firing peanut shells. At the combustor top, O_2 was (almost) independent of the fuel type but noticeably affected by EA.

Fig. 3 compares the axial CO, C_xH_y (as CH_4) and NO concentration profiles in the conical FBC between the two fuels for the range of EA. All the profiles exhibited two specific regions in the reactor, within which the net result of formation/decomposition of these gaseous compounds was quite different.

In the first region, comprising the dense and splash zones of the fluidized bed (0 < Z < 0.6 m), all the gaseous compounds showed a significant increase, mainly due to the rapid devolatilization of fuel particles followed by volatile oxidation (e.g., during formation of CO and NO), while the decomposition rate of CO, C_xH_y and NO was substantially lower. The higher reactivity and solid density of peanut shell particles led to the (i) higher devolatilization rate, i.e., higher yield of volatile-related CO, C_xH_y and nitrogenous species (the latter being affected by fuel-N), (ii) more rapid oxidation of C_xH_y and char-C (contributing to CO formation) [1], and (iii) higher NO formation rate compared to that for firing tamarind shells at similar EA. However, with increasing EA, the rate of CO and C_xH_y oxidation was apparently higher, which resulted in lower concentrations of both CO and C_xH_y in the bed region and, consequently, in their lower peak values observed at $Z \approx 0.6$ m. On the contrary, at higher EA, NO was found to be increased more rapidly (following the fuel-NO formation mechanism [1,13]), which led to the higher peaks of NO (at $Z \approx 0.6$ m) for both

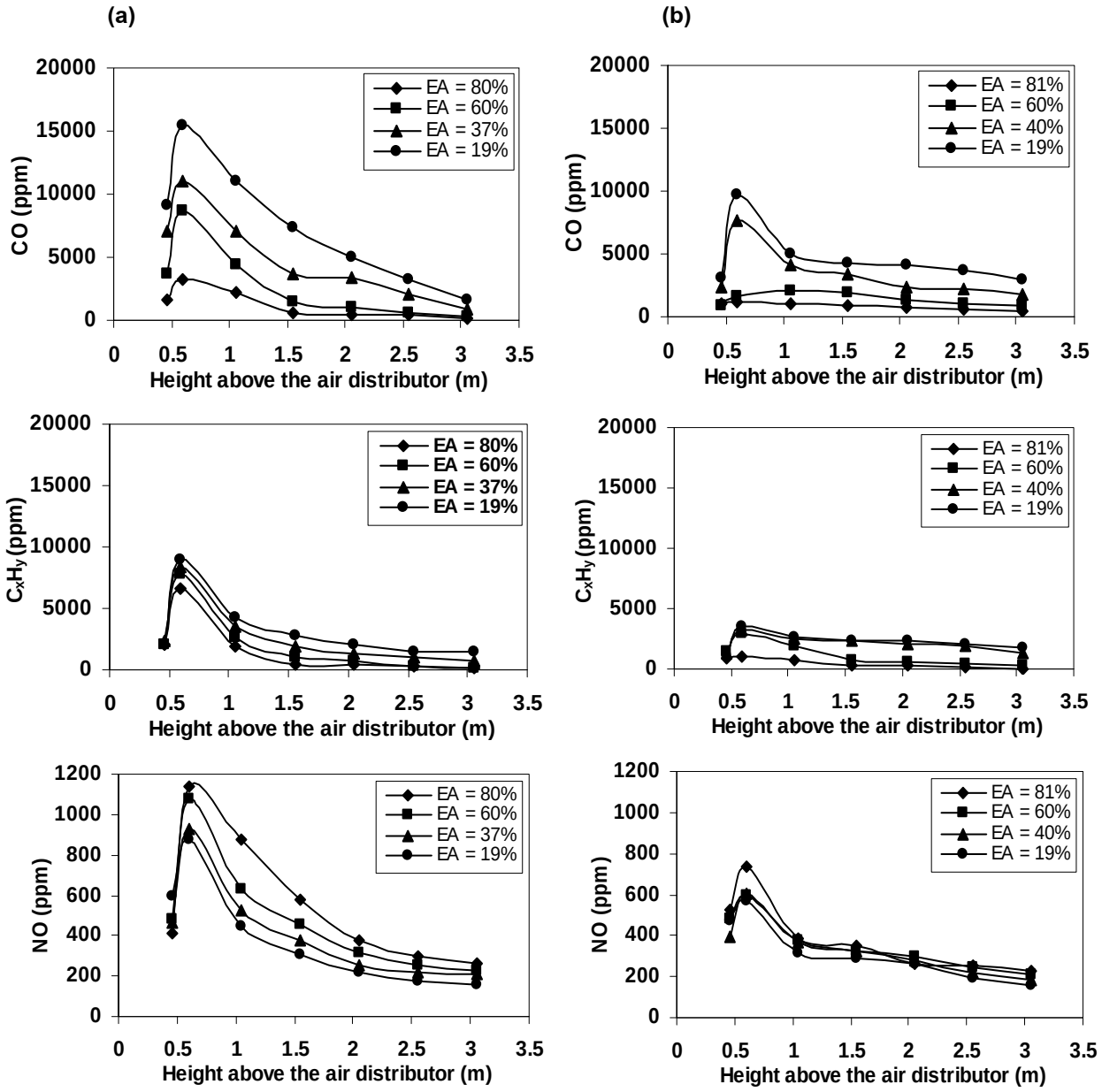

Fig. 3 Effects of excess air on the axial CO, C_xH_y (as CH_4) and NO concentration profiles in the conical FBC when firing 60 kg/hr of (a) peanut shells and (b) tamarind shells.

biomass fuels. Note that the axial gradient of NO in the first region was also affected by a catalytic reduction of NO, via its reactions with CO and C_xH_y on the surface of alumina sand and fuel-char particles [1,3].

In the second region (Z > 0.6 m), where the secondary (decomposition) reactions were predominant, all the gaseous compounds showed the trend to drop along the combustor height at a particular rate depending on fuel properties and EA. It can be seen in Fig. 3 that for the given fuel, CO, C_xH_y and NO at the combustor top were correlated with the respective concentration peaks at $Z \approx 0.6$ m, i.e., were affected by the processes in the fluidized bed. The CO oxidation (to CO_2) likely occurred via a sequence of chain chemical reactions involving O_2 and water vapor, whereas

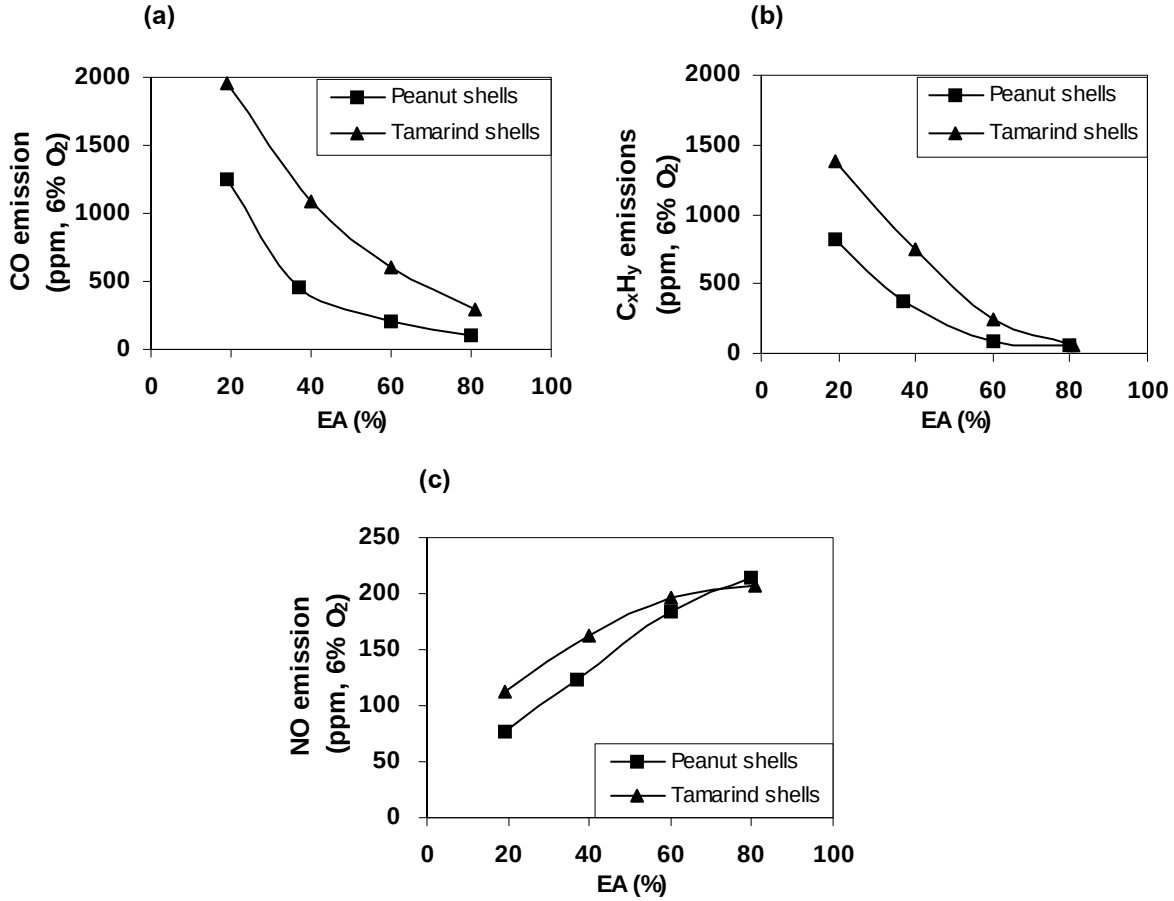

Fig. 4 Effects of the excess air on the (a) CO, (b) C_xH_y (as CH_4) and (c) NO emissions from the conical FBC when firing 60 kg/h of peanut/tamarind shells.

the decomposition of C_xH_y proceeded via two groups of intermediate reactions: the first one leading to formation of CO, and the second one being responsible for oxidation of CO to CO_2. A higher carryover of tamarind shell chars and volatiles into the freeboard, resulted in higher CO and C_xH_y at the combustor top compared to burning peanut shells at similar EA, though the peaks of CO and C_xH_y (at $Z \approx 0.6$ m) showed the opposite trend. It should be noted that the drop of NO along the axial direction in the second region was mainly caused by the above catalytic reduction (reactions) of NO on the surface of char and ash particles. However, when firing peanut shells, the reduction rate of NO in this region was substantially higher than that when firing tamarind shells (see Fig. 3). This result can be explained by higher catalytic effectiveness of fly ash as well as greater fuel ash (leading to the higher concentration of solids in the flue gas) of peanut shells compared to those of tamarind shells. Consequently, despite significant difference in the peak values of NO between the two fuels, the NO concentration at the top of the combustor firing these two fuels turned out to be roughly at a similar level, affected only by EA.

3.2 Emissions

Fig. 4 depicts the CO, C_xH_y (as CH_4) and NO emissions (all presented on dry gas basis and at 6% O_2) from the conical FBC fired

with shredded peanut/tamarind shells at the fuel feedrate of 60 kg/h for the range of EA. For the selected operating conditions, all the emissions for firing tamarind shells were somewhat higher than those for firing peanut shells.

At fixed EA, the emissions of CO and C_xH_y from the conical FBC fired with peanut shells were found to be lower than those for burning tamarind shells, though the peaks of CO and C_xH_y (at $Z \approx 0.6$ m) for the two fuels showed the opposite trends. These results can be explained by the above-mentioned elevated carryover of tamarind shell chars and volatiles into the freeboard compared to that for firing peanut shells. It appears that the CO and C_xH_y emissions can be effectively reduced/controlled by increasing EA (within the applied range) and maintaining this key operating variable at an appropriate level. To meet the national emission limit for CO (740 ppm, on dry gas basis, as corrected to 6% O_2 [14]), peanut shells can be burned at excess air of about 30% (or higher), whereas the minimum required excess air for firing tamarind shells is about 50%.

Despite the peak concentration of NO (at $Z \approx 0.6$ m) for firing peanut shells was substantially higher than that for burning tamarind shells, the NO emission from firing peanut shells turned out to be lower than that for the latter case. Such a result can be explained by the greater reduction rate of NO in the combustor freeboard, as well as in the cyclone, likely due to higher catalytic effectiveness of the peanut shell ash particles. For the range of operating conditions, the NO emission for firing both fuels met the national emission limit for NO (205 ppm, on dry gas basis, as corrected to 6% O_2 [14]). Thus, regarding to the emission requirements, the above-mentioned excess air values for CO can be applied for firing the fuels in this conical FBC, as ensuring the minimal emission of NO from the combustor.

3.3 Combustion efficiency

Table 3 shows the heat losses that are due to unburned carbon and incomplete combustion together with the combustion efficiency (all as the percentages of fuel LHV) of the conical FBC when firing the biomass fuels at

Table 3. Heat losses and combustion efficiency of the conical FBC when firing 60 kg/h biomass fuels at similar ranges of excess air.

Fuel burned	Excess air (vol. %)	Heat loss due to unburned carbon (%)	Heat loss owing to incomplete combustion (%)	Combustion efficiency (%)
Peanut shells	19	0.23	1.80	98.0
	37	0.22	0.89	98.9
	60	0.10	0.23	99.7
	80	0.10	0.13	99.8
Tamarind shells	19	0.05	2.39	97.6
	40	0.04	1.27	98.7
	60	0.05	0.79	99.2
	81	0.20	0.31	99.5

the fuel feedrate of 60 kg/h for the range of excess air. Because of the relatively low ash content in these fuels (see Table 2), the heat loss due to unburned carbon had minor effects on the heat balance, leaving the heat loss due to incomplete combustion to have a predominant role. Hence, the combustion efficiency of the conical FBC can be improved by minimizing the CO and C_xH_y emissions.

It can be seen in Table 3 that with increasing EA, the heat loss due to unburned carbon changed insignificantly, whereas the heat loss due to incomplete combustion showed the trend to be substantially reduced following the behavior of CO and C_xH_y emissions. Hence, the combustion efficiency of the conical FBC can be ensured at a high level, 98.8–99.7%, when firing both fuels at EA of 40–80%.

Taking into account the above emission characteristics and combustion efficiencies, excess air values of 40% and 60% seem to be the best options for firing peanut shells and tamarind shells, respectively, at the fuel feed rate of 60 kg/h. Under such conditions, the combustor can be operated with high combustion efficiency, about 99%, while the major emissions can be controlled at acceptable values (meeting the national emission limits): CO = 400 ppm and NO = 125 ppm for firing peanut shells, and CO = 680 ppm and NO = 190 ppm for firing tamarind shells (all these emissions are given on a dry gas basis and at 6% O_2).

4. Conclusions

The conical fluidized-bed combustor has been successfully tested for individual firing of shredded peanut and tamarind shells at the fuel feedrate of 60 kg/h, while ranging excess air from 20% to 80%. The specific conclusions derived from this study are as follow:

- the axial temperature profiles in the combustor are rather uniform indicating quasi-isothermal conditions when burning both biomass fuels;
- the axial CO, C_xH_y (as CH_4) and NO concentration profiles inside the reactor point at the occurrence of two specific regions exhibiting significant differences in the formation and decomposition of these gaseous pollutants;
- the rate of CO, C_xH_y (as CH_4) and NO formation in the fluidized bed (including the bed splash zone) is substantially affected by the solid density of fuel, as well as by the texture of fuel particles;
- due to the high catalytic effectiveness of the peanut shell ash, the emission of NO from the combustor firing this fuel is somewhat lower than that for firing tamarind shells despite the fuel-N content in peanut shells is substantially higher than in tamarind shells;
- excess air of 40% seems to be an optimum option for firing peanut shells, while 60% is more appropriate for firing tamarind shells, as ensuring the highest, about 99%, combustion efficiency of the conical FBC and acceptable level of CO and NO emissions from the combustor, both meeting the corresponding national emission limits.

5. Acknowledgements

The authors would like to acknowledge the financial support from the Thailand Research Fund (Contract No. BRG 5380015) and from the Commission on Higher Education, Ministry of Education, Thailand (Contract No. 6/2551).

6. References

[1] Werther, J., Saenger, M., Hartge, E.-U., Ogada T. and Siagi, Z. (2000). Combustion of agricultural residues, *Progress in Energy and Combustion Science*, vol. 26, pp. 1–27.

[2] Natarajan, E., Nordin, A. and Rao, A.N. (1998). Overview of combustion and gasification of rice husk in fluidized bed reactors, *Biomass and Bioenergy*, vol. 14, pp. 533–546.

[3] Permchart, W. and Kouprianov, V.I. (2004). Emission performance and combustion efficiency of a conical fluidized-bed combustor firing various biomass fuels, *Bioresource Technology*, vol. 92, pp. 83–91.

[4] Chyang C.S., Qian F.P., Lin Y.C. and Yang S.H. (2008). NO and N_2O emission characteristics from a pilot scale vortexing fluidized bed combustor firing different fuels, *Energy & Fuels*, vol. 22, pp. 1004–1011.

[5] Fang, M., Yang, L., Chen, G.., Shi, Z., Luo, Z. and Cen, K.F. (2004). Experimental study on rice husk combustion in a circulating fluidized bed, *Fuel Processing Technology*, vol. 85, pp. 1273–1282.

[6] Kaynak, B., Topal, H. and Atimtay, A.T. (2005). Peach and apricot stone combustion in a bubbling fluidized bed, *Fuel Processing Technology*, vol. 86, pp. 1175–1193.

[7] Varol, M. and Atimtay, A.T. (2007). Combustion of olive cake and coal in a bubbling fluidized bed with secondary air injection, *Fuel* vol. 86, pp. 1430–1438.

[8] Topal, H., Atimtay, A.T. and Durmaz A. (2003). Olive cake combustion in a circulating fluidized bed, *Fuel*, vol. 82, pp. 1049–1056.

[9] Khan A.A., de Jong, W., Jansens P.J. and Spliethoff H. (2009). Biomass combustion in fluidized bed boilers: Potential problems and remediates, *Fuel Processing Technology*, vol. 90, pp. 21–55.

[10] Arromdee, P., Kuprianov, V.I., Aunsakul, C., Pilthai, C., Tuenudomseel, D., Tangphong, P., Sookkasem, W. (2011). Comparative studies on combustion of peanut and tamarind shells in a bubbling fluidized bed: Fluidization characteristics of binary alumina–biomass mixtures. In *Proceedings of The Second TSME Conference on Mechanical Engineering*, 19–21 October, 2011, Krabi, Thailand (in this volume).

[11] Bezgreshnov, A.N., Lipov, Y.M. and Shleipher, B.M. (1991). Computations of Steam Boilers (in Russian), *Energoatomizdat*: Moscow.

[12] Basu, P., Cen, K.F. and Jestin L., (2000). Boilers and Burners, *Springer*, New York.

[13] Winter, L., Wartha, C. and Hofbauer, H. (1999). NO and N_2O formation during the combustion of wood, straw, malt waste and peat, *Bioresource Technology*, vol. 70, pp. 39–49.

[14] Pollution Control Department, Ministry of Natural Resources and Environment, Thailand. Air pollution standards for industrial sources. http://www.pcd.go.th/info_serv/reg_std_airsnd03.html.